The Effect of Intersymbol Interference on Error Rate in Binary Differentially-Coherent Phase-Shift-Keyed Systems

By W. M. HUBBARD

(Manuscript received March 7, 1967)

Two types of binary differentially-coherent phase-shift-keyed signals (designated AM-DCPSK and FM-DCPSK) which look attractive for high-speed digital communication systems are considered. The error rate as a function of signal-to-noise ratio is calculated for each type of signal. For the AM-DCPSK signal the effects of intersymbol interference from adjacent time slots, phase distortion in the pulses, nonideal delay lines in the differential phase detector and nonideal regeneration (in a sense described in the text) are considered. For the FM-DCPSK signal the effects of nonideal regeneration and of a degradation parameter δ are considered. The parameter δ can be readily associated with phase distortion and nonideal delay lines in the differential phase detector. By means of a straightforward but tedious calculation it can be related to intersymbol interference if the transfer characteristics of the channel are known. The results of the calculations are presented, in graphical form, for wide ranges of signal-to-noise ratio and of the parameters which describe the intersymbol interference and nonideal regenerator performance. Error rates from 10^{-10} to 10^{-4} are considered.

I. INTRODUCTION

This paper presents a summary of calculations which were performed before and during the construction of a 300-Mb/s repeater for a guided millimeter-wave communication system. Consequently, the problems which are considered are oriented toward problems which arise in connection with these high-speed systems, e.g., finite-width decision thresholds, imperfect phase shifts in the modulators, etc. Because of the nature of the channels envisioned for these systems, only

intersymbol interference from adjacent time slots is significant and the treatment of intersymbol interference will include only adjacent time-slot interference.

1.1 *Summary of Previous Results*

Several authors[1,2,3,4] have calculated the error rate as a function of signal-to-noise ratio, S/N, for an ideal differentially-coherent phase-shift-keyed (DCPSK) system, i.e., a system in which intersymbol interference can be ignored and in which regeneration is assumed to be ideal. The well-known result is

$$\Pi_0 = \tfrac{1}{2} \exp(-\mathrm{S/N}), \tag{1}$$

where Π_0 is the probability of error for the ideal case. The author[5] has considered the effects of nonideal regeneration. Sections II and III of this paper extend these error-rate calculations to include the effects of intersymbol interference for two types of DCPSK signals. These signals are discussed and compared in the next paragraph.

1.2 *Comparison of AM-DCPSK and FM-DCPSK Signals*

In a DCPSK system the information is carried in the phase of the signal at the sampling point in one time slot relative to the phase of the signal at a time, T, earlier where T is the reciprocal of the bit rate B. This phase change can be accomplished in several ways; the effect of intersymbol interference depends on how it is accomplished. In the following, two types of modulation which can be thought of as limiting cases (in a sense that should become clear in the following discussion) will be considered.

The first type to be considered consists of a sequence of amplitude modulated RF pulses occurring at the bit rate, B. The information is carried in whether the relative carrier phase between adjacent pulses is 0 or π. Since a phase shift of π radians is equivalent to a change in sign, the signal can be written in the form

$$S(t) = \sum_{n=0}^{\infty} a_n S_0(t - nT) \exp(j\omega_0 t), \tag{2}$$

where $a_n = +1$ or -1 according to whether the phase in the nth time slot is 0 or π, respectively. $S_0(t - nT)$ is a pulse-shaping term which reaches its maximum value at $t = nT$. Intersymbol interference arises from the fact that $S_0(t - nT)$ is not confined to a single time slot. Fig. 1(b) is an example of this type of signal.

Since the signal $S(t)$ in (2) is in fact a pure AM signal (even though

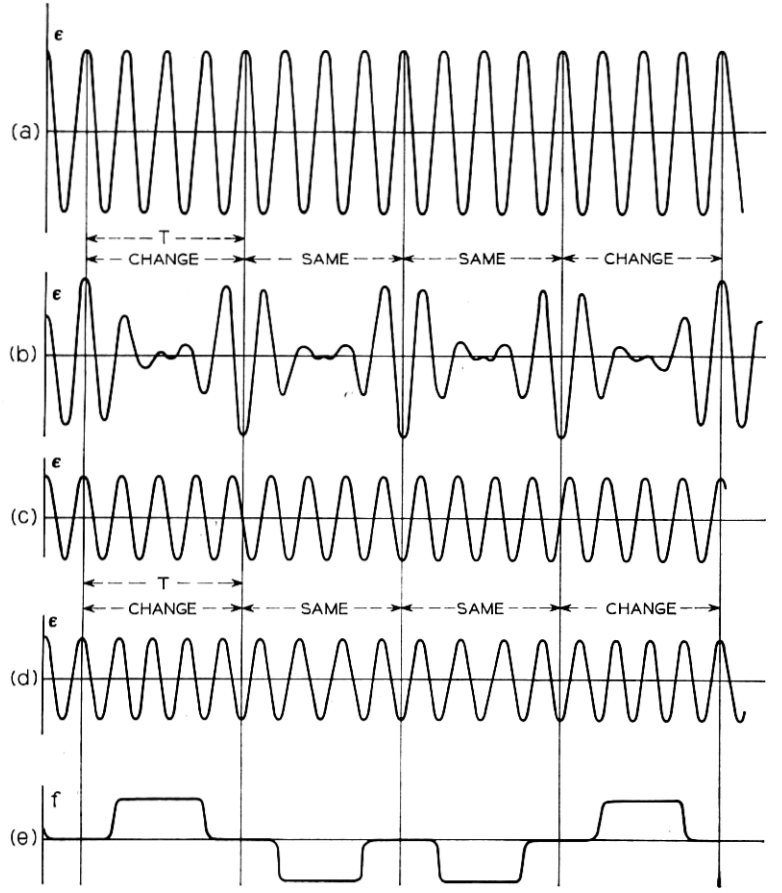

Fig. 1 — (a) Unmodulated IF-carrier for AM-DCPSK; (b) idealized AM-DCPSK signal; (c) unmodulated IF-carrier for FM-DCPSK; (d) idealized FM-DCPSK signal carrying the same information as in (b); (e) frequency vs time for the signal in (d).

the information is recovered by comparing phases) this type of modulation can be designated AM-DCPSK in order to distinguish it from a second type which will be described below. Error rate as a function of S/N for an AM-DCPSK signal with intersymbol interference and non-ideal regeneration is calculated in Section II.

The second type of modulation consists of a constant amplitude signal which shifts phase between sampling points by means of a frequency swing. This signal, which can be designated FM-DCPSK,

can be written in the form

$$S(t) = \exp j\left\{\omega_0 t + \int_0^t \omega(t')\,dt'\right\}, \quad \text{where} \quad \int_{(n-1)T}^{nT} \omega(t')\,dt' = \alpha_n \tag{3}$$

and α_n is a chance binary variable (which contains the information being transmitted) that can take on any two values which differ by π. In practice, the values $+\pi/2$ and $-\pi/2$ offer certain advantages so the following discussion will assume, for clarity, that $\alpha_n = \pm\pi/2$. This assumption is unnecessary for the calculation and does not influence the result in any way. An example of this type of signal is given in Fig. 1(d).

Error-rate vs S/N for an FM-DCPSK signal with intersymbol interference and nonideal regeneration is calculated in Section III.

1.3 *The Differential Phase Detector*

Both AM-DCPSK and FM-DCPSK signals can be detected using a product demodulator of the type shown in Fig. 2. For this device to function properly, the intermediate frequency f_0 and the bit rate, B, must be related according to

$$f_0 = \tfrac{1}{2}mB \qquad m = 1, 2, 3, \cdots \quad \text{for} \quad \text{AM-DCPSK} \tag{4}$$

and

$$f_0 = \tfrac{1}{2}(m + \tfrac{1}{2})B \qquad m = 1, 2, 3, \cdots \quad \text{for} \quad \text{FM-DCPSK.} \tag{5}$$

When these conditions are satisfied for the appropriate type of modulation, the output of the differential phase detector will be pro-

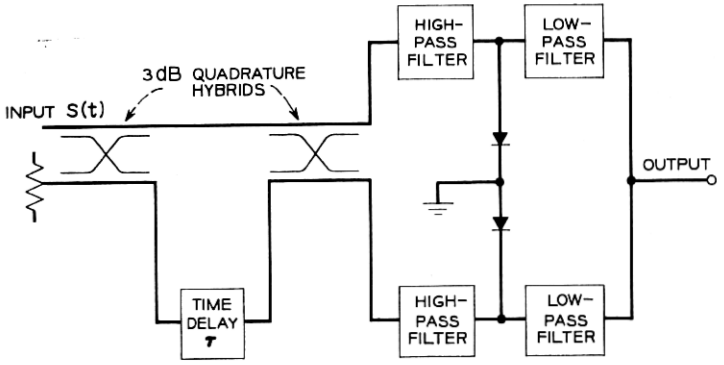

Fig. 2 — Differential phase detector.

portional to V, where

$$V = [(\mathbf{u} + \mathbf{v})^2 - (\mathbf{u} - \mathbf{v})^2] = uv \cos \psi. \tag{6}$$

Here $\mathbf{u}$ is a vector which represents the amplitude and phase of the signal at time t, $\mathbf{v}$ the amplitude and phase at time $t-T$, and ψ is the phase difference between times t and $t-T$.

1.4 *The Regenerator*

The output of the differential phase detector is fed into the regenerator where it is sampled at a particular point in each time slot. An ideal regenerator would regenerate a $+1$ if $\cos \psi > 0$ and a -1 if $\cos \psi < 0$ regardless of how small $|\cos \psi|$ might be. Since no realizable regenerator will accomplish this, we take as a model of a regenerator a device which regenerates $+1$'s and -1's according to the following inequalities:

$$\begin{aligned} +1 \quad &\text{if} \quad 1 \geqq \cos \psi \geqq \epsilon \\ -1 \quad &\text{if} \quad -\epsilon \geqq \cos \psi \geqq -1 \end{aligned} \tag{7}$$

$+1$ or -1 randomly and with equal probability if $|\cos \psi| < \epsilon$.

It is convenient to define a threshold T in terms of the parameter ϵ by means of the relation

$$\mathrm{S/T} = -20 \log \epsilon \; dB.$$

The quantity S/T is the so-called signal-to-threshold ratio and represents the ratio of the expected value of signal power to the minimum value of signal power which will cause the regenerator to function reliably (in the absence of noise).

In high-speed systems the signal-to-threshold ratio is limited by practical considerations (at the present state of the art) to values of the order of 10 dB or less.

II. ERROR-RATE WITH AM-DCPSK MODULATION

2.1 *Intersymbol Interference*

The voltages at the two output ports of the second quadrature hybrid in Fig. 2 will at any instant consist of contributions from the following sources:

(*i*) The two pulses being compared.
(*ii*) Intersymbol interference from other pulses in the channel.

(*iii*) Interchannel interference from other channels propagating in the medium.
(*iv*) Noise.

The following assumptions are made:

(*i*) The noise is Gaussian and the noise on adjacent pulses is statistically independent.*
(*ii*) Interchannel interference is negligible.
(*iii*) Intersymbol interference comes only from adjacent pulses.
(*iv*) The sampling is accomplished instantaneously.

Since the phases of these output voltages are, in general, different we must represent these voltages by vectors (in a plane). Consider four adjacent pulses labeled LABR from left to right. The pulses labeled A and B are the two whose phases are to be compared. The ones labeled L and R are significant because they contribute to the intersymbol interference. Let **L**, **A**, **B**, and **R** be vectors of unit magnitude which lie along the $+X$ or $-X$ direction. Let ρ_a represent the ratio of $S_0(T)$ to $S_0(0)$ and ρ_r the ratio of $S_0(-T)$ to $S_0(0)$ where $S_0(t)$ is the quantity introduced in (2). Let **a** and **b** represent the noise on pulses A and B, respectively.

The outputs $\mathbf{r}_2$ and $\mathbf{r}_1$ of the two output ports of the second quadrature hybrid are then

$$\mathbf{r}_2 = \mathbf{S} + \mathbf{a} + \mathbf{b} = \mathbf{u} + \mathbf{v} \tag{8}$$

$$\mathbf{r}_1 = \mathbf{D} + \mathbf{a} - \mathbf{b} = \mathbf{u} - \mathbf{v}, \tag{9}$$

respectively, where

$$\mathbf{S} = \mathbf{A} + \mathbf{B} + \rho_a(\mathbf{B} + \mathbf{R}) + \rho_r(\mathbf{L} + \mathbf{A}) \tag{10}$$

$$\mathbf{D} = \mathbf{A} - \mathbf{B} + \rho_a(\mathbf{B} - \mathbf{R}) + \rho_r(\mathbf{L} - \mathbf{A}). \tag{11}$$

For a given pulse pattern **S** and **D** are determined. The quantities **a** and **b** represent four independent Gaussian variables with zero means and equal variances.

Consider first the means of the distributions of $\mathbf{r}_2$ and $\mathbf{r}_1$. Since **a** and **b** are Gaussian variables of zero mean these means are determined for a given pulse pattern by **S** and **D**, respectively.

There are $2^4 = 16$ possible patterns for the four pulses, L, A, B, and

* The latter assumption is never strictly true since the noise is band-limited. It has been shown,[6] however, that the effects of this correlation on error rate are negligible unless the noise bandwidth is smaller than about 1.4 times the bit-rate.

TABLE I

Case	L	A	B	R	$\frac{1}{2}S$	$\frac{1}{2}D$	$\frac{1}{4}(S^2 - D^2) = \frac{1}{4}PP_d$ (neglecting terms in ρ^2)
1	1	1	1	1	$1 + \rho_a + \rho_r$	0	$1 + 2\rho_a + 2\rho_r$
2	1	1	1	−1	$1 + \rho_r$	ρ_a	$1 + 2\rho_r$
3	−1	1	1	1	$1 + \rho_a$	$-\rho_r$	$1 + 2\rho_a$
4	−1	1	1	−1	1	$\rho_a - \rho_r$	1
5	1	1	−1	1	ρ_r	$1 - \rho_a$	$-1 + 2\rho_a$
6	1	1	−1	−1	$-\rho_a + \rho_r$	1	−1
7	−1	1	−1	1	0	$1 - \rho_a - \rho_r$	$-1 + 2\rho_a + 2\rho_r$
8	−1	1	−1	−1	$-\rho_a$	$1 - \rho_r$	$-1 + 2\rho_r$

R. Of these, eight can be obtained by reversing *all* of the phases in each of the other eight patterns. Since such a sign reversal has no effect on the error probabilities to be considered only eight patterns need be considered. These are numerated in Table I.

We now consider the output of the differential phase detector for an arbitrarily chosen pulse pattern. The criterion for making the decision as to whether the pulses are of the same phase or of opposite phase is that of determining whether

$$V = \{|\mathbf{r}_2|^2 - |\mathbf{r}_1|^2\} \tag{12}$$

is positive or negative. This criterion is equivalent to deciding whether the phase angle between the received pulses (including crosstalk and noise) is less than 90 degrees or greater than 90 degrees, respectively. It is worth mentioning that due to the correlation between the signals in the sum and difference arms 0 would in general not be the proper decision level if the phases of the pulse tails relative to the pulse peaks were fixed and known. Since this is probably not going to be the case in any reasonable system, the decision level will be taken at 0 in this calculation. (Zero is the optimum decision level for random phase in the tails.)

With the assumptions that have been made, the error probability including the effects of intersymbol interference can be determined by a straightforward extension of the calculation due to Bennett and Salz.[3] Substituting (8) and (9) into (12) gives

$$V = (P + x)(P_d + x_d) + yy_d\,, \tag{13}$$

where

$$P = S + D \qquad P_d = S - D$$
$$x = 2a_x \qquad x_d = 2b_x$$
$$y = 2a_y \qquad y_d = 2b_y\,.$$

Equation (13) is identical in form to (54) of Ref. 3. However, the symbols now include the effects of intersymbol interference. Following the method of Bennett and Salz[3] one obtains for the probability of error

$$\Pi = \frac{1}{\pi}\int_0^{\pi/2} \exp\left(-\frac{P^2P_d^2}{8\sigma^2(P_d^2\cos^2\theta + P^2\sin^2\theta)}\right) d\theta. \tag{14}$$

It must be recalled that P and P_d are pulse-pattern dependent. For a random message the error rate is obtained by averaging the expression in (14) over the eight possible values of P and P_d.

In order to determine the worst possible error rate for any arbitrary message, we can evaluate Π for the worst pulse pattern. From Table I it is apparent that this is Case 7 if there is no phase distortion in the pulse tails. In any event this case represents an upper limit on the error rate. Fortuitously, since $S = 0$ in this case, P^2 is equal to P_d^2 and the integral for Π becomes particularly simple.

$$\Pi = \frac{1}{\pi}\int_0^{\pi/2} \exp\left(-\frac{P^2}{8\sigma^2}\right) d\theta = \frac{1}{2}\exp\left[-\frac{(1-\rho_a-\rho_r)^2}{2\sigma^2}\right]. \tag{15}$$

Thus, the effects of intersymbol interference can be treated, for the worst pulse pattern at least, as a degradation of the signal-to-noise ratio by the amount

$$20\log(1-\rho_a-\rho_r)\ \text{dB}.$$

The extension of this calculation to the case where both intersymbol interference and a finite-width decision threshold[5] are present is straightforward. One replaces the integral in (90) of Ref. 3:

$$\int_0^\infty dz\int_{-\infty}^{\infty}\int_{-\infty}^{\infty} p(-z \mid x, y)g(x, y)\,dx\,dy,$$

by the sum of two integrals:

$$\frac{1}{2}\int_{-4\epsilon}^{4\epsilon} dz\int_{-\infty}^{\infty}\int_{-\infty}^{\infty} p(-z \mid x, y)q(x, y)\,dx\,dy + \int_{4\epsilon}^{\infty} dz\int_{-\infty}^{\infty}\int_{-\infty}^{\infty} p(-z \mid x, y)g(x, y)\,dx\,dy.$$

These integrals are then evaluated by the method used in Appendix A of Ref. 5. Figs. 3, 4, and 5 show error rate as a function of signal-to-noise ratio in the case where ρ_a equals ρ_r in terms of signal-to-threshold ratio and crosstalk per tail. In these figures $\rho_T = \rho_a = \rho_r$ is expressed in dB.

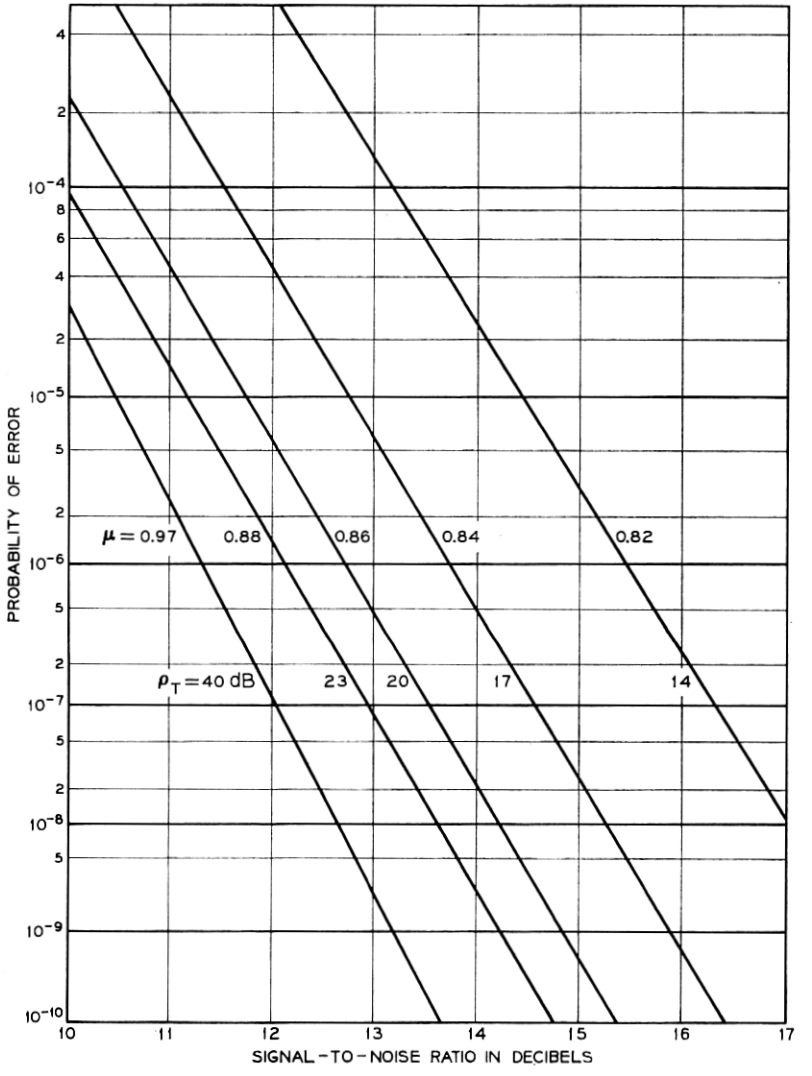

Fig. 3 — Probability of error vs signal-to-noise ratio for S/T = 15 dB AM-DCPSK.

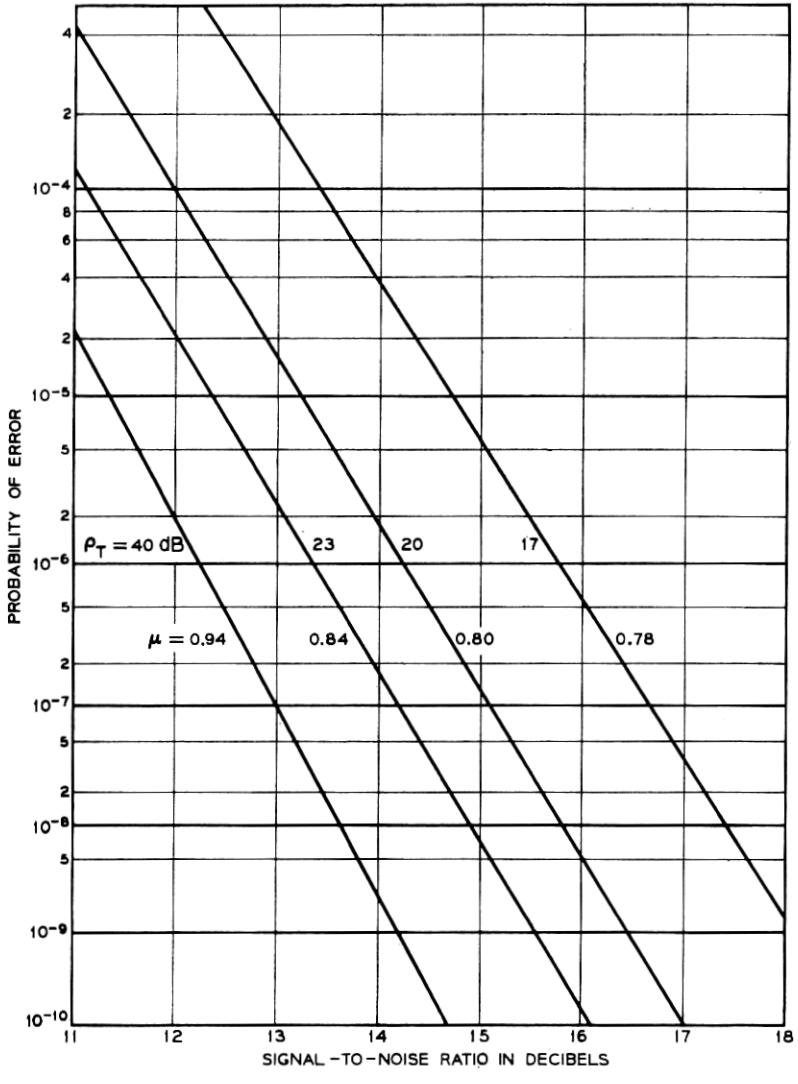

Fig. 4 — Probability of error vs signal-to-noise ratio for S/T = 9 dB AM-DCPSK.

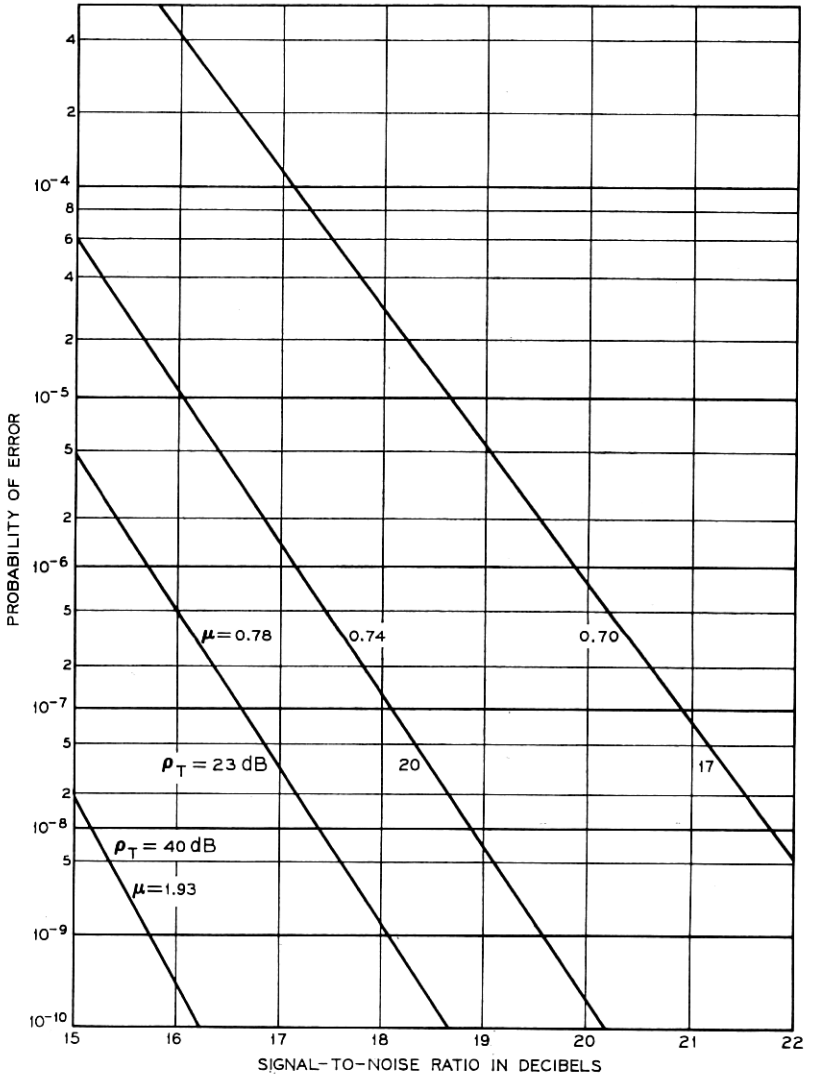

Fig. 5 — Probability of error vs signal-to-noise ratio for S/T = 6 dB AM-DCPSK.

The scale of the ordinate in Figs. 3, 4, and 5 is chosen such that a plot of Π_0 vs S/N from (1) gives a straight line. One finds from inspection of Figs. 3, 4, and 5 that even in the presence of intersymbol interference and nonideal regeneration, this linearity persists. The slope of the line does change, however. Fig. 6 shows the slope, μ, of these lines as a function of S/T for various values of ρ_T. Here the slope, μ, is defined such that $\mu = 1$ for the ideal case [see (1)].

2.2 *Phase Distortion*

In an AM-DCPSK system there are two important types of phase distortion which are readily treated by a modification of the foregoing calculation. One type is representable by a phase shift of the pulse in the nth time slot by β degrees relative to the phase which should have been transmitted in that time slot. In this case the vectors **B**, and ρ_n**B**, in (10) and (11) are rotated an amount β. This could arise, for example, from an improperly balanced pulse modulator. In the other type of phase distortion all of the delayed pulses in the differential phase detector are shifted an amount φ relative to their proper value. In this case the vectors **B**, ρ_r**A**, and ρ_n**R** are rotated an amount φ. This could arise, for example, from a delay line of improper length in the differential phase detector.

The analysis of these effects constitutes a straightforward extention of the calculation in paragraph 2.1 and only the results will be given here. Fig. 7 shows the degradation in error-rate performance which results from a phase shift β for $\rho_T = -\infty$, -26, and -20. This effect is virtually independent of S/T for S/T $>$ 6 dB. Fig. 8 shows the

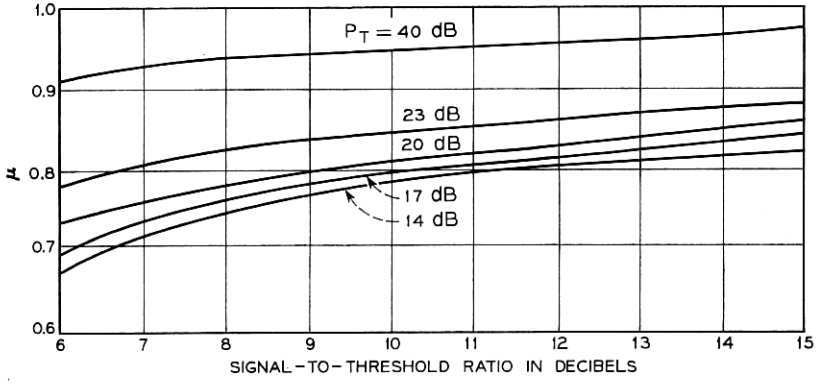

Fig. 6 — Slope, μ, of error probability vs S/N curve as a function of S/T.

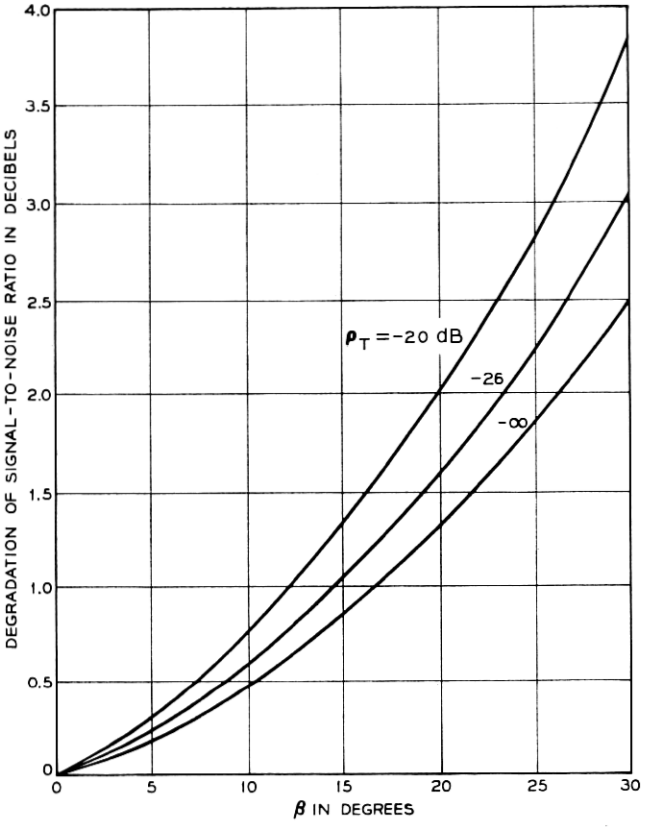

Fig. 7 — Degradation in signal-to-noise ratio due to a phase shift, β, in one of the received pulses.

degradation for phase shift φ. The result is virtually independent of S/T for S/T $>$ 6 dB and of ρ_T for $\rho_T < -20$ dB.

III. ERROR-RATE IN AN FM-DCPSK SYSTEM

In an FM-DCPSK system, it is useful to include a limiter in the receiver after the noise has been added. Therefore, the following calculation assumes that an ideal limiter is used. By ideal limiter is meant a device which receives at its input the signal

$$A(t) \exp [j\varphi(t)]$$

and at its output delivers the signal

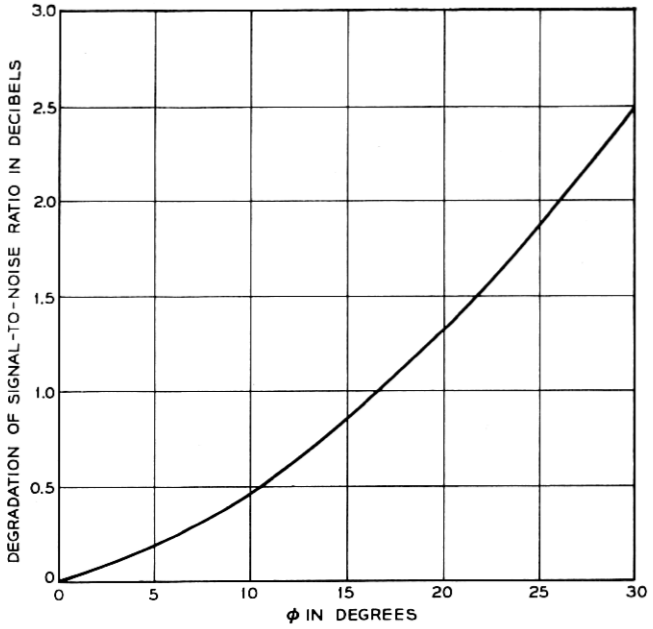

Fig. 8 — Degradation in signal-to-noise ratio due to improper delay line length.

$$A_0 \exp [j\varphi(t)].$$

Since the amplitudes u and v in (6) are constants after limiting, the output of the differential phase detector is simply

$$V = \cos \psi$$

and the error probability is directly related to the probability density of ψ.

The intersymbol interference is assumed to manifest itself in the form of a perturbation in the phase of the signal at the sampling time. More precisely, the intersymbol interference (in this model) introduces a (pattern dependent) phase shift δ_n so that the phase change in the nth time slot is $\pm(\pi/2 + \delta_n)$ instead of $\pm\pi/2$.

The value of δ_n (for each distinct pulse pattern) depends on the details of the signal waveform and the transfer function of the devices in the system. The determination of the δ_n's for particular systems is beyond the scope of this paper. For a discussion of this problem see, for example, Rice and Bedrosian.[7] This paper concerns itself with the

effect on error rate of a particular value of δ_n. In order to apply these results to the performance of a particular system, one needs to compute the values of δ_n for the various pulse patterns and then average these computed error rates over the possible pulse patterns.

The parameter δ can also be used to investigate the effects of phase distortion and nonideal delay lines in the differential phase detector just as β and φ were used in the AM-DCPSK case. One need only associate δ with the total (net) phase shift for these distortions (including that due to intersymbol interference).

Let α_0 and β_0 represent the phase shift due to intersymbol interference (and any other degradation in phase) on the two pulses being compared. This situation is represented by the phasor diagram in Fig. 9. Following the method described in Ref. 5, one obtains for the probability density function of ψ

$$
\begin{aligned}
p(\psi) = {} & \frac{1}{2\pi} \exp\left(-1/\sigma^2\right) + \frac{1}{\pi} \exp\left(-1/2\sigma^2\right) \\
& - \frac{1}{4\pi\sigma^2} \int_{-\pi/2}^{\pi/2} \cos(\alpha - \alpha_0) \cos(\alpha + \psi - \beta_0) \\
& \cdot \exp\left[-\frac{\sin^2(\alpha - \alpha_0) + \sin^2(\alpha + \psi - \beta_0)}{2\sigma^2} \right] d\alpha \\
& + \frac{1}{4\pi\sigma^2} \int_{-\pi/2}^{\pi/2} \cos(\alpha - \alpha_0) \cos(\alpha + \psi - \beta_0) \\
& \cdot \exp\left[-\frac{\sin^2(\alpha - \alpha_0) + \sin^2(\alpha + \psi - \beta_0)}{2\sigma^2} \right] \\
& \cdot \operatorname{erf} \frac{\cos(\alpha - \alpha_0)}{\sqrt{2}\sigma} \operatorname{erf} \frac{\cos(\alpha + \psi - \beta_0)}{\sqrt{2}\sigma} \, d\alpha. \qquad (16)
\end{aligned}
$$

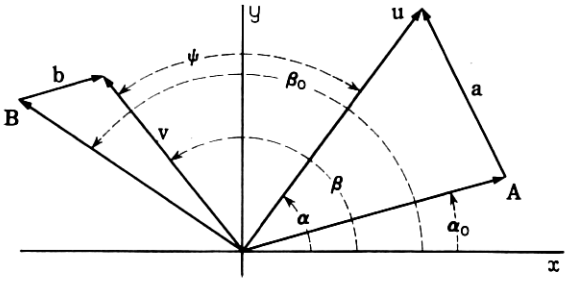

Fig. 9 — Phasor diagram for the differential detection process.

From the regenerator model (Paragraph 1.4) one observes that an error is made if $\cos \psi \geqq \epsilon$ and there is a 50-percent probability of error if $| \cos \psi | < \epsilon$. The error probability, Π, is therefore given for a transmitted signal which should result in $\psi = \pi$ by

$$\Pi = \int_{-\theta}^{\theta} p(\psi)\, d\psi + \frac{1}{2}\int_{\theta}^{\pi-\theta} p(\psi)\, d\psi + \frac{1}{2}\int_{\pi+\theta}^{-\theta} p(\psi)\, d\psi, \qquad (17)$$

where

$$\theta = \cos^{-1} \epsilon \qquad 0 \leqq \theta \leqq \pi/2.$$

Substituting (16) into (17) gives, after some simplification,

$$\Pi = \frac{1}{2} - \frac{1}{4\pi\sigma^2}\int_{-1}^{1}\int_{y_l(x)}^{y_u(x)} \exp\left(-\frac{x^2+y^2}{2\sigma^2}\right) dy\, dx, \qquad (18)$$

where

$$y_u(x) = \sqrt{1-x^2}\cos(\varphi - \delta) + x \sin(\varphi - \delta)$$

$$y_l(x) = -\sqrt{1-x^2}\cos(\varphi + \delta) + x \sin(\varphi + \delta)$$

$$\delta = \alpha_0 - \beta_0\,, \qquad \varphi = \frac{\pi}{2} - \theta = \sin^{-1}\epsilon.$$

Now $y_u(x)$ and $y_l(x)$ are segments of (different) ellipses both of which have the following properties: They are centered at the origin, have their major axes along the line $x = y$, and are tangent to the lines $x = 1$, $x = -1$, $y = 1$, and $y = -1$. A typical pair of such ellipses is shown in Fig. 10. By symmetry the small area A in Fig. 10(a)

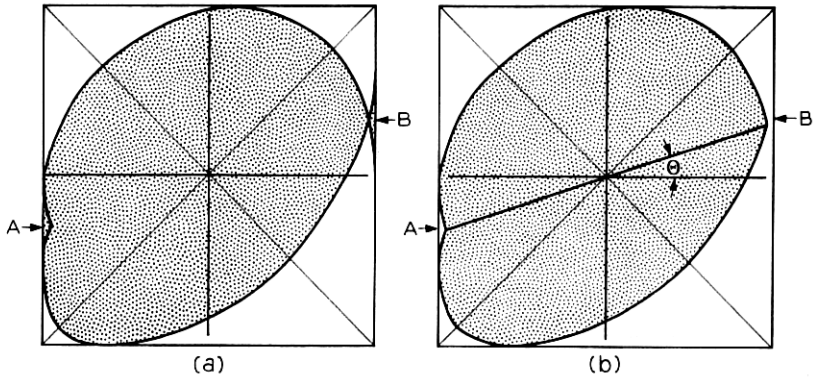

Fig. 10 — Region of integration in (16).

is equal to the small area B. Therefore, due to the spherical symmetry of the integrand, the integration indicated by the limits $-1 \leqq x \leqq 1$, $y_l(x) \leqq y \leqq y_u(x)$ [as shown by the shaded portion of Fig. 10(a)] can be replaced by the limits which correspond to integrating over the region bounded by the upper ellipse and the line $\theta = \Theta$ and the region bounded by the lower ellipse and this same line [see Fig. 10(b)]. Writing the integral in polar coordinates, one obtains a form which is easily integrated over r. When this is done, the following result is obtained:

$$\Pi = \frac{1}{4\pi}\left\{\int_{\Theta}^{\Theta+\pi} \exp\left\{-\frac{\cos^2(\varphi-\delta)}{2\sigma^2[1-\sin(\varphi-\delta)\sin 2\theta]}\right\} d\theta + \int_{\Theta+\pi}^{\Theta} \exp\left\{-\frac{\cos^2(\varphi+\delta)}{2\sigma^2[1-\sin(\varphi+\delta)\sin 2\theta]}\right\} d\theta\right\}. \tag{19}$$

But these integrals are periodic in period π, therefore, the Θ's can be deleted. The error rate can then be written

$$\Pi = \tfrac{1}{2}P_0(\varphi+\delta) + \tfrac{1}{2}P_0(\varphi-\delta), \tag{20}$$

where

$$P_0(\Phi) = \frac{1}{2\pi}\int_{-\pi/2}^{\pi/2} \exp\left(-\frac{\cos^2\Phi}{2\sigma^2[1-\sin\Phi\sin\theta]}\right) d\theta. \tag{21}$$

This integral is not soluble in closed form. The integral

$$P(\Phi) = \frac{1}{2\pi}\int_{-\pi/2}^{\pi/2} \exp\left(-\frac{\cos^2\Phi}{2\sigma^2}[1+\sin\Phi\sin\theta]\right) d\theta$$

is soluble and is a good approximation to $P_0(\Phi)$ over a wide range of values of σ and Φ. It can be written

$$P(\Phi) = \frac{1}{2}\exp\left(-\frac{\cos^2\Phi}{2\sigma^2}\right) I_0\left(\frac{\cos^2\Phi\sin\Phi}{2\sigma^2}\right)$$

where I_0 is the modified Bessel function of the first kind. A complete consideration of the accuracy of this approximation is quite tedious and will not be considered further because $P_0(\varphi)$ itself is so readily obtained by numerical integration of (21).

Fig. 11 shows $P(\varphi)$ for several values of S/N. Figs. 12, 13, 14, and 15 show Π(S/N) for S/T $= \infty$, 12, 9, 6 dB, respectively, for $\delta = 0$, 5, 10, and 15 degrees.

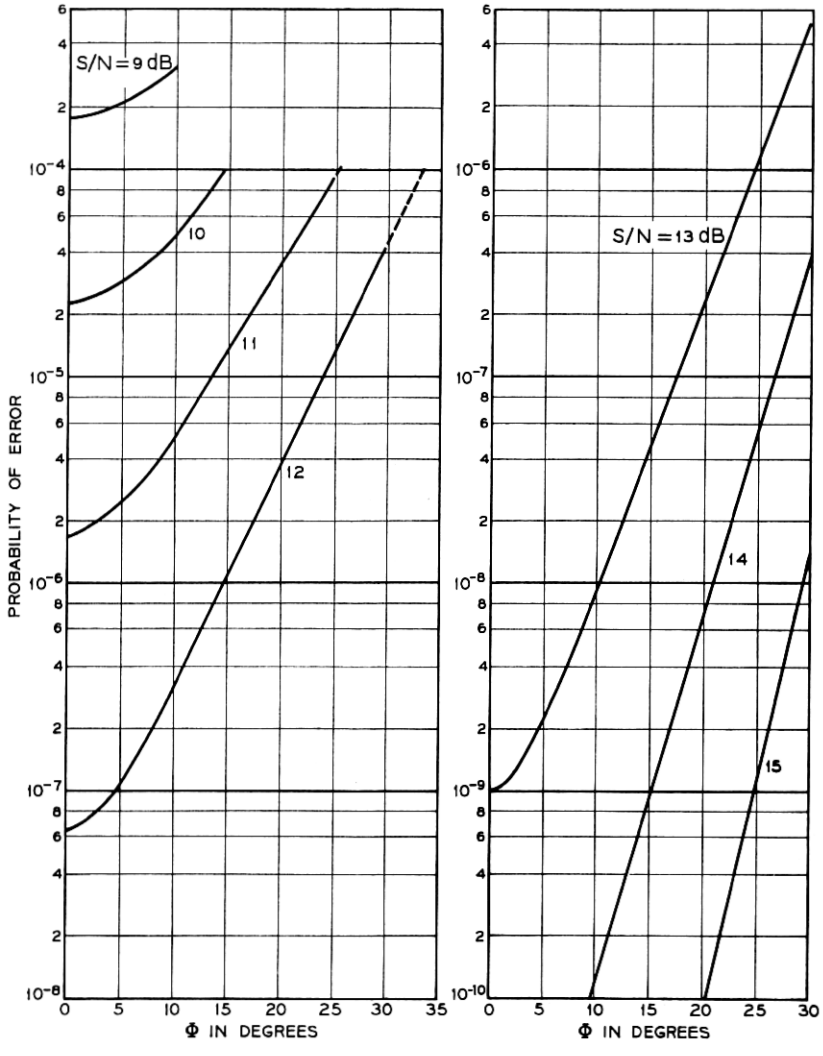

Fig. 11 — Numerical evaluation of the error-rate integral.

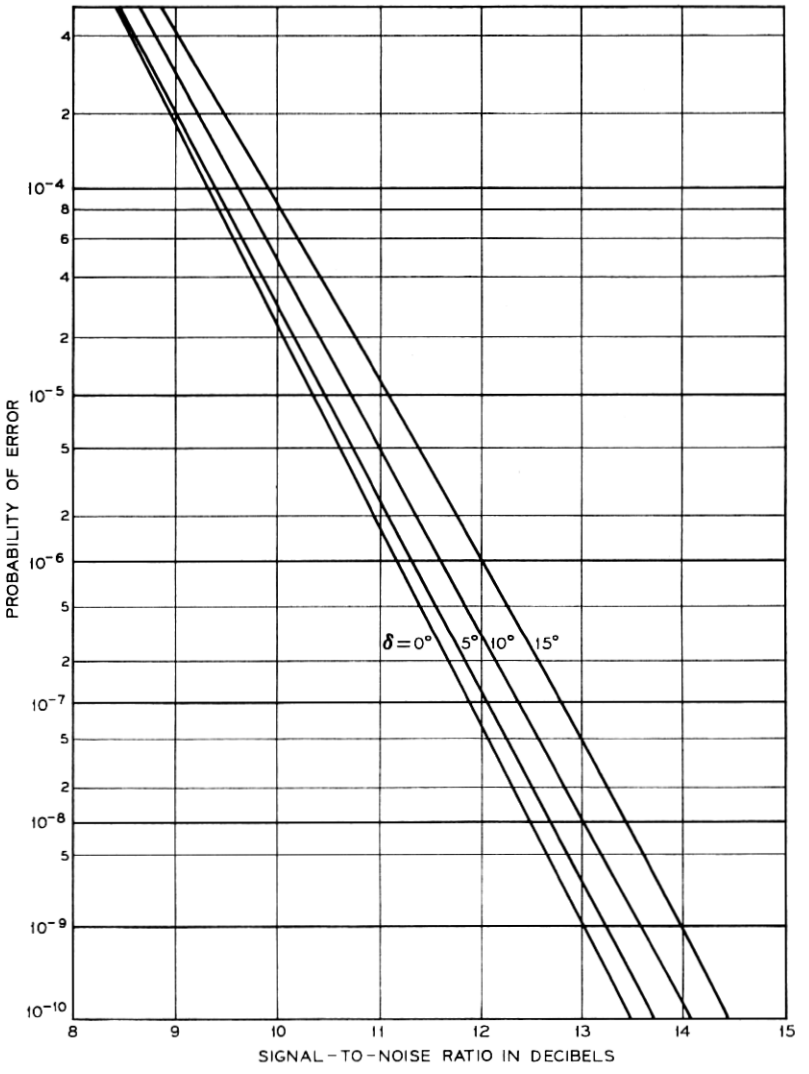

Fig. 12 — Probability of error vs signal-to-noise ratio for S/T = ∞ FM-DCPSK.

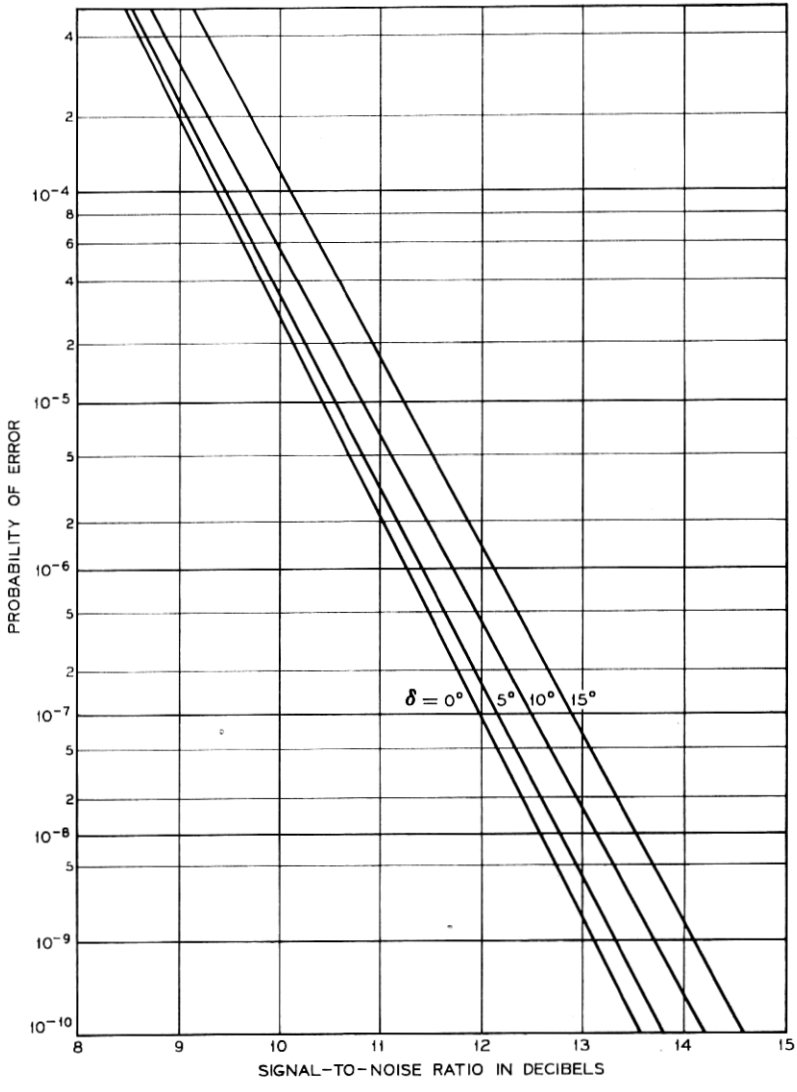

Fig. 13 — Probability of error vs signal-to-noise ratio for S/T = 12 dB FM-DCPSK.

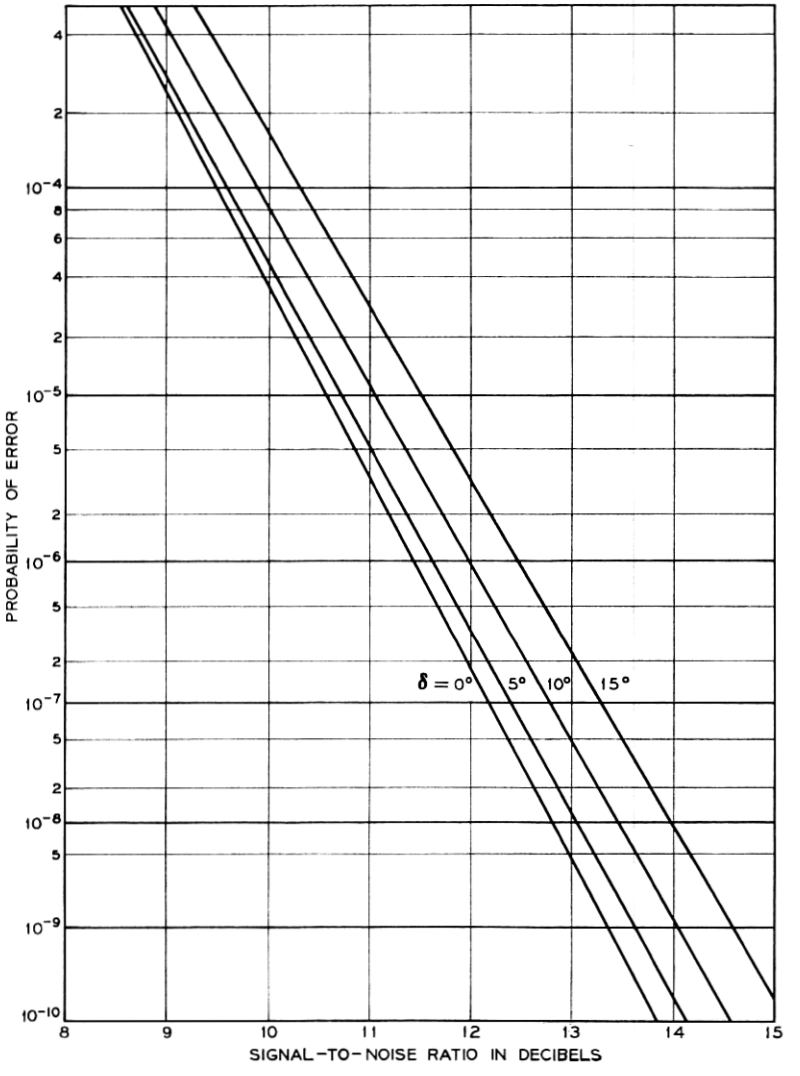

Fig. 14 — Probability of error vs signal-to-noise ratio for S/T = 9 dB FM-DCPSK.

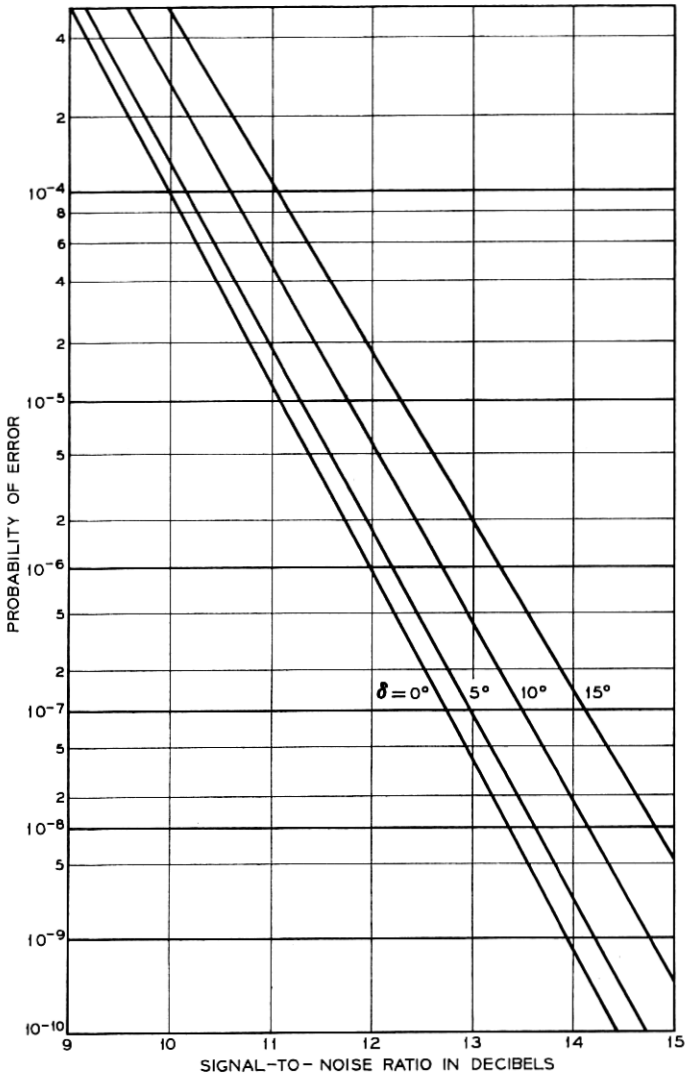

Fig. 15 — Probability of error vs signal-to-noise ratio for S/T = 6 dB FM-DCPSK.

V. ACKNOWLEDGMENTS

The author is grateful to Mrs. C. L. Beattie and Mrs. E. Kerschbaumer for programming the numerical calculations and to Mr. W. D. Warters for numerous enlightening conversations during the course of the calculations.

APPENDIX

Description of the Operation of the Differential Phase Detector for an FM-DCPSK Signal

The differential phase detector is shown in Fig. 2. For an FM-DCPSK signal with no noise or distortion the input is given by (3). One can readily show that the signals in the output ports of the second 3-dB quadrature hybrid are given by

$$A(t) = \tfrac{1}{2}\cos\left\{\omega_0 t + \int_{-\infty}^{t}\omega(t')\,dt'\right\} - \tfrac{1}{2}\cos\left\{\omega_0(t-\tau) + \int_{-\infty}^{t-\tau}\omega(t')\,dt'\right\}$$

$$B(t) = \tfrac{1}{2}\sin\left\{\omega_0 t + \int_{-\infty}^{t}\omega(t')\,dt'\right\} - \tfrac{1}{2}\sin\left\{\omega_0(t-\tau) + \int_{-\infty}^{t-\tau}\omega(t')\,dt'\right\}.$$

If the detectors, mounted as shown in Fig. 2, are regarded as having square-law behavior, the output is given by

$$\begin{aligned} V(t) &\propto B^2(t) - A^2(t) \\ &\propto \tfrac{1}{2}\cos\left\{\omega_0\tau + \int_{t-\tau}^{t}\omega(t')\,dt'\right\} + \text{terms in } 2\omega_0 t. \end{aligned}$$

The terms in $2\omega_0 t$ are removed by the low-pass filters. We can thus write the basic equation of the differential phase detector for a FM-DCPSK signal as

$$V(t) = \cos\left\{\omega_0\tau + \int_{t-\tau}^{t}\omega(t')\,dt'\right\}. \tag{22}$$

For use as a differential phase detector one chooses $\tau = T =$ the reciprocal of the bit rate, and an IF such that $\omega_0 T = (m+\frac{1}{2})\pi$ where m can be any integer. This equation then becomes

$$V(t) = \sin\left\{\int_{t-T}^{t}\omega(t')\,dt'\right\},$$

which by (3) must be

$$V(t) = \sin\alpha_n = \pm 1$$

at the sampling points $t = nT$.

REFERENCES

1. Lawton, J. G., Comparison of Binary Data Transmission, Proc. 1958 Conf. Mil. Electron.
2. Cahn, Charles, R., Performance of Digital Phase Modulation Communication Systems, IRE Trans. *CS*, May 1959, pp. 3–6.
3. Bennett, W. R. and Salz, J., Binary Data Transmission by FM Over a Real Channel, B.S.T.J., *42*, September, 1963, pp. 2387–2426.
4. Bussgang, J. J. and Leiter, M., Error-Rate Approximation for Differential Phase Shift Keying, IEEE Trans. *CS-12*. March, 1964. pp. 18-27.
5. Hubbard, W. M., The Effect of a Finite-Width Decision Threshold on Binary Differentially Coherent PSK Systems, B.S.T.J., *45*, February, 1966, pp. 306–320.
6. Hubbard, W. M., Effect of Noise Correlation on Binary Differentially Coherent PSK Communication Systems, B.S.T.J., *46*, January, 1967, pp. 277–280.
7. Bedrosian, E. and Rice, S. O., Distortion and Crosstalk of Linearly Filtered and Angle-Modulated Signals, unpublished work.